

## Time-Resolved Particle Velocity Measurements at Impact

Velocities of 10 km/s CONF-981109--

M. D. Furnish, L.C. Chhabildas, W.D. Reinhart

Sandia National Laboratories

Albuquerque, NM 87185-1181

RECEIVED

JUN 30 1998

OSTI

Hypervelocity launch capabilities (9 -16 km/s) with macroscopic plates have become available in recent years. It is now feasible to conduct instrumented plane-wave tests using this capability. Successfully conducting such tests requires a planar launch and impact at hypervelocities, appropriate triggering for recording systems, and time-resolved measurements of motion or stress at a particular point or set of points within the target or projectile during impact. We have conducted the first time-resolved wave-profile experiments using velocity interferometric techniques at impact velocities of 10 km/s. These measurements show that aluminum continues to exhibit normal release behavior to 161 GPa shock pressure, with complete loss of strength of the shocked state. These experiments have allowed a determination of shock-wave window transparency in conditions produced by a hypervelocity impact. In particular, lithium fluoride appears to lose transparency at a shock stress of 200 GPa; this appears to be the upper limit for conventional wave profile measurements using velocity interferometric techniques.

DISTRIBUTION OF THIS DOCUMENT IS UNLIMITED

### 1. INTRODUCTION

#### Plane Wave Experiments

Plane-wave impacts have been utilized using explosive or smooth bore systems for many

MASTER

\* Sandia is a multiprogram laboratory operated by Sandia Corporation, a Lockheed Martin Company for the US Department of Energy under contract DE-AC04-94AL85000.

## **DISCLAIMER**

This report was prepared as an account of work sponsored by an agency of the United States Government. Neither the United States Government nor any agency thereof, nor any of their employees, makes any warranty, express or implied, or assumes any legal liability or responsibility for the accuracy, completeness, or usefulness of any information, apparatus, product, or process disclosed, or represents that its use would not infringe privately owned rights. Reference herein to any specific commercial product, process, or service by trade name, trademark, manufacturer, or otherwise does not necessarily constitute or imply its endorsement, recommendation, or favoring by the United States Government or any agency thereof. The views and opinions of authors expressed herein do not necessarily state or reflect those of the United States Government or any agency thereof.

## **DISCLAIMER**

**Portions of this document may be illegible electronic image products. Images are produced from the best available original document.**

years to measure material properties under shock loading. A suite of diagnostic and experimental techniques [1,2] are used to measure material properties in the high-pressure, high-temperature shocked state induced in materials resulting from impact. These techniques allow measurements of the shock-Hugoniot [3], shock-loading and release behavior [4,5], material strength [3-7], shock-induced melting [5, 8-9], and shock-induced vaporization [8-9] processes in materials. The measurement of these material properties forms a data base to develop constitutive models to represent material behavior in dynamic loading [10].

Until approximately six years ago, the highest pressure and temperature states achieved in material by gun impact loading techniques were restricted to those available with two-stage light-gas guns [11-13]. The most extreme conditions were those produced using high impedance impactor materials such as tantalum or platinum at impact velocities of 8 km/s.

There is a need, however, to determine the equations of state of materials in regimes of extreme high pressures, temperatures and strain rates that are not attainable on current two-stage light-gas guns. These regimes are dominated by phase changes such as melting or vaporization. Some key areas of interest include these transitions, other aspects of the equation-of-state (Hugoniot, thermal properties such as the Grüneisen parameter), and meteorite impact phenomenology. Conventional two-stage light-gas guns, however, have limited accessibility to such extreme thermodynamic states.

### Hypervelocity Launcher

Sandia National Laboratories has recently developed a hypervelocity launcher (HVL) capable of launching 0.5 mm to 1.0 mm thick by 6 mm to 19 mm diameter plates to velocities approaching 16 km/s. This new launcher complements the available suite of high-pressure, high-temperature loading techniques (examples of radiative sources are lasers, Z-pinches,

etc.,) currently being used at various laboratories to determine the EOS of weapon and ICF materials at extreme thermodynamic states.

It is the purpose of this paper to report recent results of velocity interferometer (VISAR [14]) particle-velocity measurements of shock loading and release in aluminum and titanium at impact velocities of  $\sim 10$  km/s using the Sandia HVL. Shock loading and release experiments on aluminum at 1.62 Mbar resulting from symmetric impact at 10 km/s indicate complete melt in the shocked state. This is evidenced both by the lack of shear strength and release wave speed measurement that is indicative of a bulk wave velocity at 1.62 Mbar.

A similar measurement with a symmetric tantalum experiment showed an abrupt loss of returned light to the velocity interferometer, VISAR, upon passage of the shock wave into the lithium fluoride window. Although this experiment failed to return the desired tantalum EOS information, it provided an important indication of the limits of VISAR methods using lithium fluoride as the window material with hypervelocity impact experiments.

## 2. HYPERVELOCITY LAUNCHER (HVL)

### Basic Operation

The principle of operation of the Sandia HyperVelocity Launcher (HVL) is briefly described here. In its simplest representation, a two stage projectile is impacted on a flyer plate, which is thus launched at a velocity of order twice the that of the incident projectile. Very high driving pressures (tens or hundreds of GPa) accelerate flier plates to hypervelocities. This loading pressure pulse on the flier plates must be time-dependent to prevent the plate from melting or vaporizing. This is accomplished by using graded-density impactors [6-7,15]. When this graded-density material is used to impact a flier-plate in a modified two-stage light gas gun, as

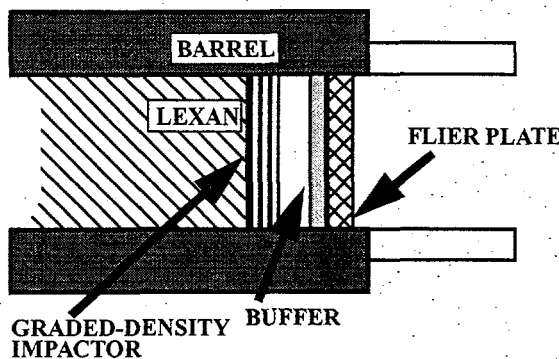


Figure 1(a). The Hypervelocity Launcher (HVL). Configuration used to launch flier plates to hypervelocities.

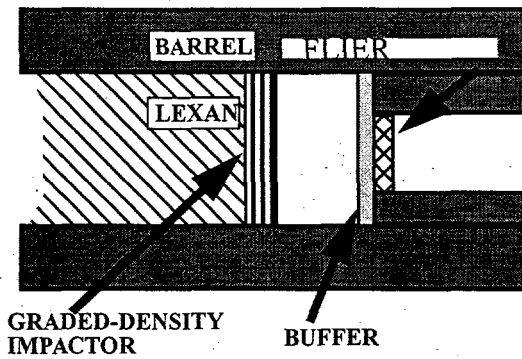


Figure 1(b). Enhanced Hypervelocity Launcher, (EHVL). Configuration used to launch confined flier plates in a tungsten barrel to hypervelocities.

indicated in Figure 1(a), nearly shockless, megabar pressures are introduced into the flier plate [7,15-18]. The pressure pulse is tailored to prevent spallation of the flier-plate.

This technique has been used [17-18] to launch nominally 1-mm-thick aluminum, magnesium and titanium (gram-size) intact plates to 10.4 km/s and 0.5-mm-thick aluminum and titanium (half-gram size) intact plates to 12.2 km/s. More recently the technique has been enhanced by using the experimental configuration described in Figure 1(b) to allow the launching of titanium and aluminum plates to velocities approaching 16 km/s [16,19]. The experimental design shown in Figure 1(b) acts as a dynamic acceleration reservoir which further enhances the flier plate velocity [16]. This is the highest mass-velocity capability attained with laboratory launchers to date, and therefore should open up investigations into new regimes of impact physics using various diagnostic tools [1-2].

#### Flyer Plate Issues

Following launch, the flyer plate must be relatively flat and cool for successful planar impact experiments. Due to the severe loading conditions which result from time-dependent megabar loading pressures, the flier plate achieves peak velocities over acceleration distance of tens of

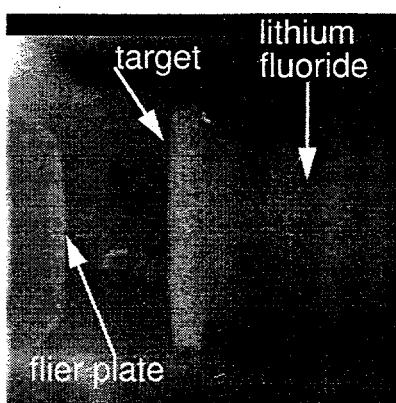


Figure 2(a). Radiograph of a titanium flier plate (prior to impacting a titanium target). The flier-plate is traveling at 9.60 km/s

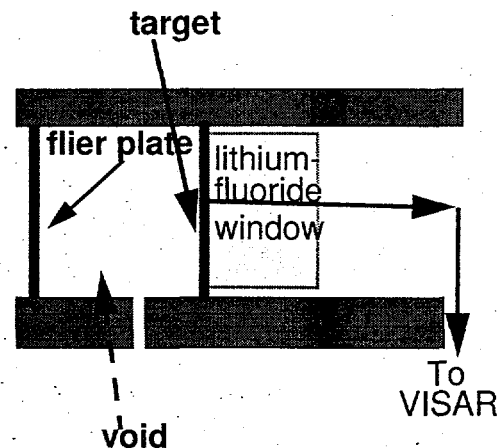


Figure 2(b). HVL configuration for shock-loading and release experiments. Resultant loading and release is measured as particle-velocity history at the target lithium fluoride window interface.

millimeters. The plate appears to be "flat" for approximately the first thirty millimeter flight distances (see Figure 2(a)). Even though shockless loading conditions are used to accelerate the flier plate, the final temperature of the flier plate upon acceleration in these studies is approximately 600 K for the geometry used in Figure 1(a) after achieving velocities of 10 km/s. This is "cold" compared to its melt temperature, despite using enormous energy (compared to its melt and vaporization energy) to achieve hypervelocities. Designs using lower-impedance buffers such as foam can further reduce the temperature of the accelerating flier-plate.

### 3. SHOCK LOADING AND RELEASE EXPERIMENTS

We have used the hypervelocity launcher (HVL) to perform one-dimensional plate-impact experiments. To achieve one-dimensional conditions, the target plate is stationed  $\sim 20$  mm from the flier-plate. This ensures that the flier plate achieves peak particle velocity prior to impact, and remains relatively flat (see Figure 2) prior to impact. No attempt has been made to date to characterize the *planarity* of the impacting flier plate. The experimental configuration used to perform shock-loading and release measurements is shown in Figure 2(b)

Recent HVL Experiments - Wave Profile Measurements

Symmetric plate-impact experiments have been performed using aluminum, titanium, and tantalum at impact velocities of  $\sim 10$  km/s. Figure 2(a) shows the radiograph of an experiment in which a 0.56 mm titanium alloy (Ti-6Al-4V) flier-plate is launched at 9.6 km/s prior to impacting a 2.0 mm thick titanium alloy target. The lithium-fluoride window[20] is clearly seen in the radiograph in Figure 2(a). The flat portion of the flier-plate prior to impact as observed in the radiograph is 19 mm. Note that for the full duration of the experiments there is a void behind the flier-plate; this allows measurements of a complete release from the shocked state. As indicated in Figure 2, a VISAR is used to estimate the particle-velocity history at the sample/lithium-fluoride window interface. The time-resolved particle velocity history measurements at the target/lithium-fluoride window interface are shown in Figure 3(a) and 3(b) for aluminum and titanium, respectively. Since no fiducial was established in these experiments, the shock arrival time at the target/window-interface is determined by impedance-match calculations based on the Hugoniots of Table 1.

**Table 1: Aluminum and Titanium Hugoniots**

Material	$C_0$ (km/s)	S	$\rho_0$ (gm/cm <sup>3</sup> )	Reference
6061-T6 aluminum	5.386	1.339	2.697	[21]
Titanium - 6Al- 4V	4.99	1.05	4.426	[22]

Wave Profile Interpretations

Figure 3(a) depicts the shock loading and release profile in aluminum shocked to 1.61 Mbar at an impact velocity of 9.95 km/s. In this experiment, a 0.98 mm thick aluminum flier-plate impacts a 1.98 mm thick aluminum target. Notice that a sustained shock of approximately 80 ns is observed in the figure prior to release. The titanium alloy is shocked to 2.3 Mbar at an

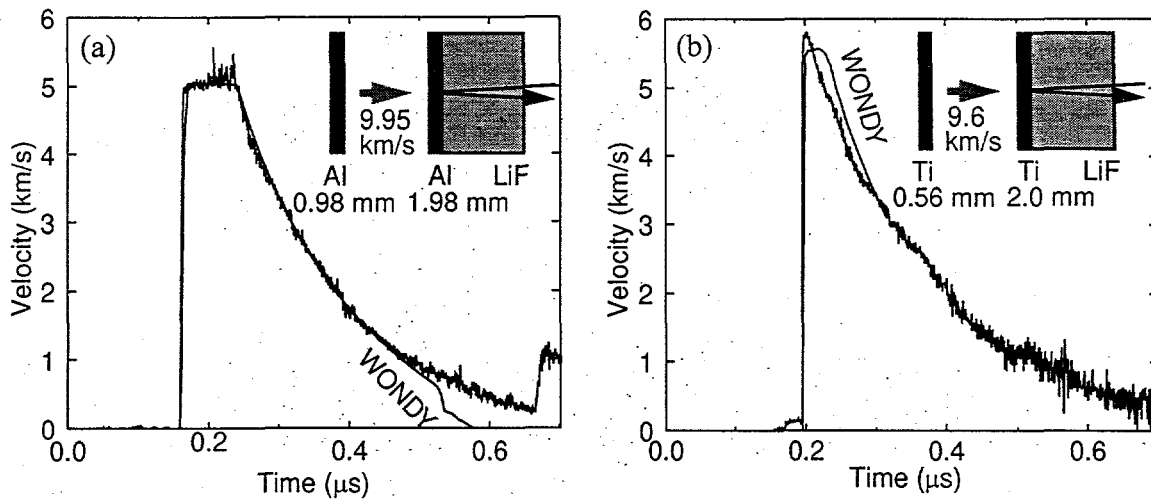


Figure 3. Measured interface particle velocity history for shock-loading and release experiments in (a) 6061-T6 aluminum at an impact velocity of 9.95 km/s, and (b) Ti-6Al-4V alloy at an impact velocity of 9.6 km/s. Symmetric impact configuration was used in both experiments. An analogous experiment with tantalum did not yield usable particle velocity history data because the LiF window became opaque (see Section 4)

impact velocity of 9.6 km/s, and a complete release profile as indicated in Figure 3(b) is measured. A profile resembling wave attenuation is measured in the titanium experiment because a thin flier plate (0.56 mm) impacts a thick (2.0 mm) target. Both experiments indicate a lack of elastic-plastic release structures—a clear indication of complete melt. These release structures then determine the off-Hugoniot states of materials shocked to extremely high-pressure.

#### Aluminum Experiments

Results of the aluminum experiment are juxtaposed on those of three analogous lower-velocity experiments [5] in Figure 4. An elastic-plastic signature is visible on the three lower-velocity wave profiles, but is not visible for the HVL experiment. This is indicated by the double-corner appearance of the beginning of the release in the profiles from tests A1, A3 and A5. Complete melt is indicated for the shocked state at 1.61 MBar. The shock Hugoniot state is based on measurements of the impact velocity and the existing equation of state for aluminum (Table 1) given by the shock-velocity ( $U_s$ )-particle ( $u_p$ ) velocity relation as ( $U_s = 5.386 \text{ (km/s)} + 1.339 u_p$ ). Inasmuch as the impact is symmetric, the particle velocity is  $u_p = 4.975 \text{ km/s}$ ,

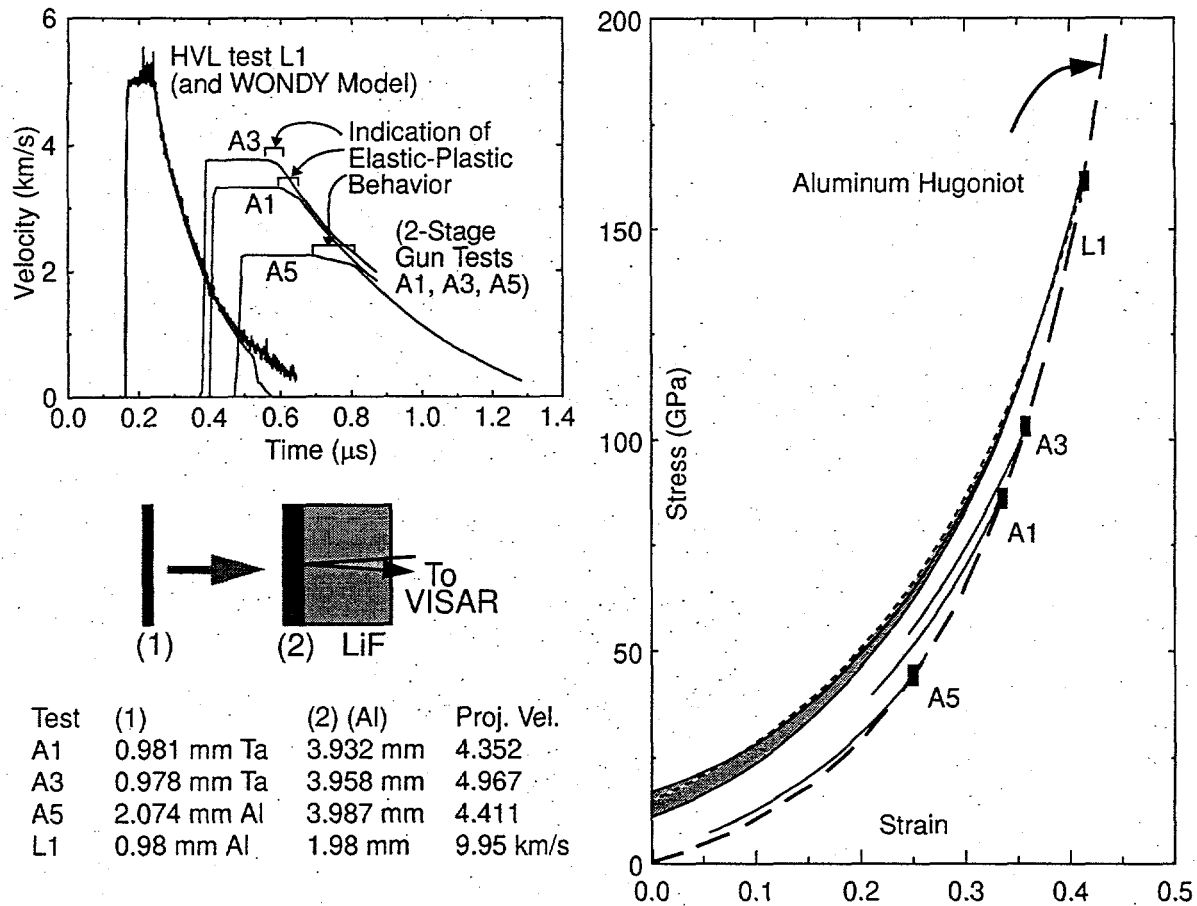


Figure 4. Wave profiles and results of Lagrangian analysis for four tests with aluminum targets (3 using 2-stage gun, L1 using HVL). All tests yielded Hugoniots lying above the Hugoniot. Shaded area represents uncertainty in L1 release due to uncertainty in LiF  $\Delta v/v_0$  (see Section 4).

giving a shock velocity  $U_s = 12.05$  km/s, a compression  $\rho/\rho_0 = 1.703$  and a stress  $P = \rho_0 U_s u_p = 161$  GPa.

#### Release paths

We have calculated release paths by several means. First, the wave profiles were analyzed by an explicit Lagrangian calculation comparing input and output wave profiles for the sample. The incremental form of the release is calculated using  $d\sigma = \rho_0 C du$  and  $d\varepsilon = du/C$ , where  $C$  is the Lagrangian wave velocity for the corresponding particle velocity decrement  $du$  at particle velocity  $u$ . Impedance mismatch calculations are also performed to transform the particle velocity measurement at the window interface to *in situ* material velocity. This analysis

yielded tabular relations between wave speed, stress, strain, strain rate, particle velocity, window velocity and time. Here, time is referenced to impact time for loading waves and to the centering time of the release in the sample for unloading waves.

Second, the Lagrangian wavecode WONDY-V [23] was used to model the experiment, with the Grüneisen  $\gamma$  adjusted to give agreement between the observed and model waveforms. A second WONDY calculation using a rate-dependent strain-hardening model (Asay and Chhabildas, [4 - 5]) produced comparable results.

#### Release Wave Velocity in Aluminum

The leading edge of the release wave velocity (traveling at the sound speed in the shocked state at 1.61 Mbar) can be calculated knowing the sample and impactor dimensions, the dwell time of the shock at the sample-window interface, and the impact velocity. The calculation method is indicated in Figure 5. The calculated Eulerian value of  $10.7 \pm 0.15$  km/s agrees very well with extrapolation of previous sound speed measurements by Asay and Chhabildas [4,5] and McQueen *et al* [24]. and is shown in Figure 6.

#### Titanium Experiment

In this symmetric impact experiment, a thin flyer plate (0.56 mm, vs. 0.98 mm for the above

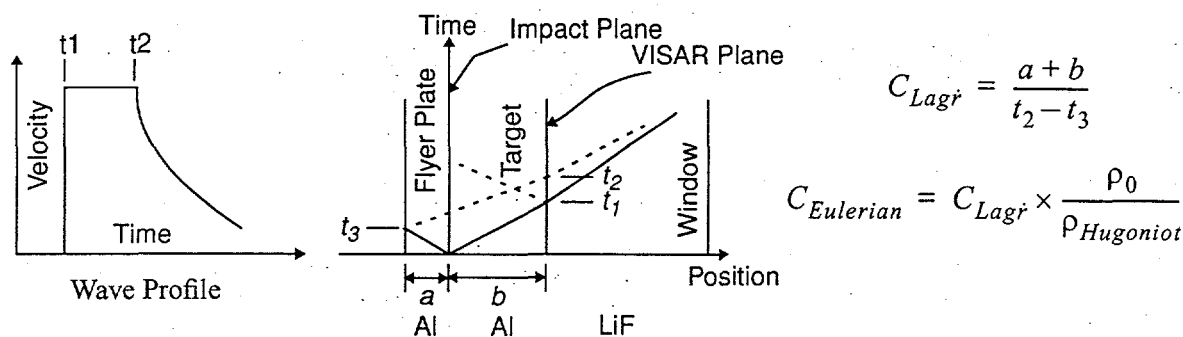


Figure 5. Method for calculating sound velocities at Hugoniot state. Times  $t_1$  and  $t_2$  are observed;  $t_3$  must be calculated from known flyer plate thickness and Hugoniot shock velocity. Lagrangian sound velocity is referenced to original part dimensions; Eulerian is referenced to compressed part dimensions and corresponds to Figure 6(b) velocities.

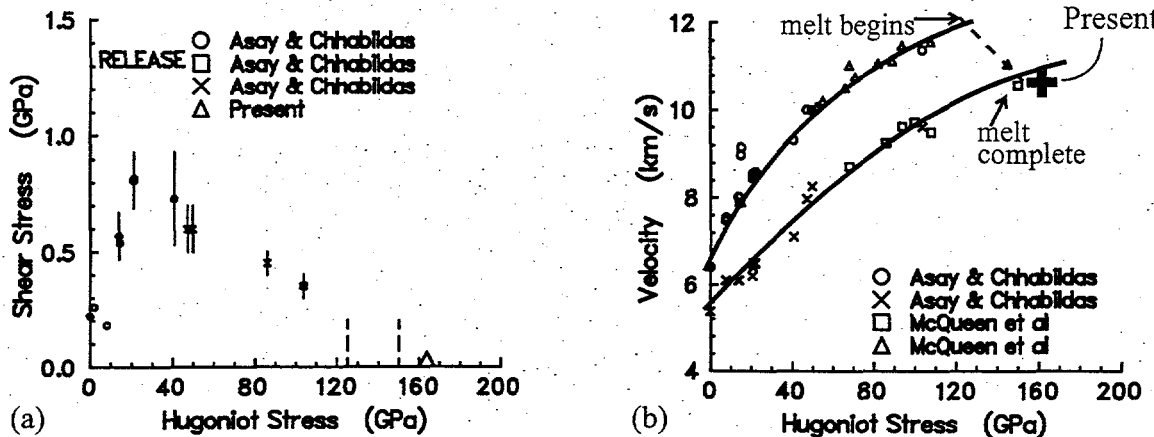


Figure 6. Measurements of (a) shear stress and (b) sound speed at 162 GPa in aluminum as determined from the release wave profile indicated in Figure 4 (a). Comparison with previous studies by Asay and Chhabildas [4,5] and McQueen et al [23] is also indicated.

aluminum experiment) impacted a titanium sample 2 mm thick. At the sample/window interface, the leading edge of the release from the back of the flyer plate had overtaken the initial loading wave. Hence an attenuating wave was observed at the window interface. This complicates the process of extracting equation-of-state information from the experiment, such as the release paths and sound velocities deduced above for the aluminum experiment L1.

In retrospect, however, had a thicker flyer plate been used to obtain an unattenuated wave, the experiment would have not yielded release profiles due to loss of VISAR fringe contrast because of limitations of the LiF window (see discussion in next section).

#### 4. LITHIUM FLUORIDE WINDOW - OPTICAL PROPERTIES

##### Transparency

The successful measurements shown in Figure 4 demonstrate the transparency of the lithium-fluoride (LiF) window at much higher pressures (and temperatures) than this window material has ever been subjected to before [20], *i.e.*, to 1.5 Mbar and 2.0 Mbar, respectively, in the aluminum and titanium experiment. A previous study had demonstrated the transparency

of LiF windows to stresses of 1.2 Mbar [20]. A symmetric impact experiment at 8.62 km/s using both tantalum as a target and as a flier plate, however, did not yield a release profile measurement similar to those in Figure 4. This corresponds to a stress of  $\sim 6.4$  Mbar in tantalum and  $\sim 2.4$  Mbar in the LiF window. This pressure level causes an apparent transparency loss in the LiF window. This is indicated in Figure 7.

The beam intensity monitor suggests that at the 1.6 Mbar stress level there is no loss of transparency, yielding extremely good fringe data at the sample-LiF window interface. As the stress level is increased to 1.97 Mbar in the window there is considerable decrease in the beam intensity signal, but nevertheless reasonable fringe information is determined at the sample window interface. At a stress level of 2.4 Mbar in the window material there is an abrupt loss of beam intensity and a total loss of fringe information from the sample/window interface. A total loss of contrast suggests a reflection from the shock front. In short, the window interferometry technique using lithium fluoride windows is restricted for use up to shock stresses of 2 Mbar in the window material. These results also point to the need to develop new time-

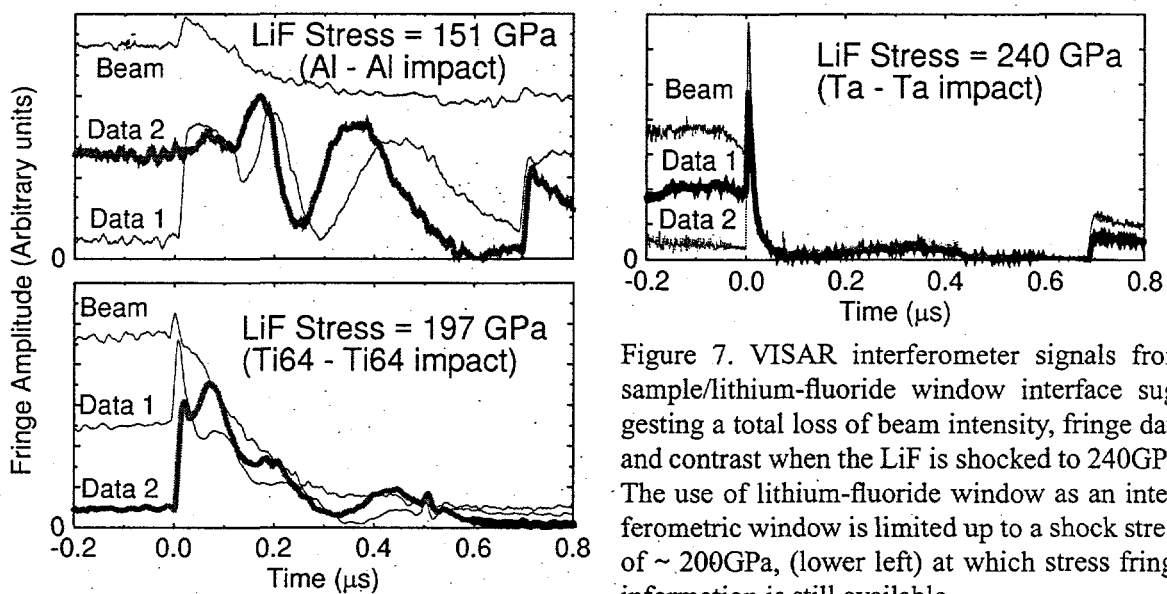


Figure 7. VISAR interferometer signals from sample/lithium-fluoride window interface suggesting a total loss of beam intensity, fringe data and contrast when the LiF is shocked to 240GPa. The use of lithium-fluoride window as an interferometric window is limited up to a shock stress of  $\sim 200$ GPa, (lower left) at which stress fringe information is still available.

resolved techniques and/or new window materials to allow successful measurements of off-Hugoniot states at extremely high pressures.

Index of Refraction

The calibration of the velocity-per-fringe sensitivity of a VISAR depends on the optical properties of the window through the frequency correction  $\Delta v/v_0$  [14] according to:

$$VPF = \frac{\lambda_0}{2\tau(1 + \delta)(1 + \Delta v/v_0)} \quad \begin{aligned} \delta &\equiv \text{Etalon dispersion correction} \\ \tau &\equiv \text{Relative delay in delay leg} \\ \lambda_0 &\equiv \text{unshifted laser wavelength} \end{aligned} \quad \text{Eq. 1.}$$

The index of refraction of a shock window material may be calculated [19] as:

$$n_H = \frac{1}{1 - \varepsilon_H} [n_0 - \varepsilon_H(1 + \Delta v/v_0)] \quad \begin{aligned} \varepsilon_H &\equiv \text{Strain at Hugoniot} \\ n_0 &\equiv \text{Ambient index of refraction} \\ \Delta v/v_0 &\equiv \text{frequency correction} \end{aligned} \quad \text{Eq. 2.}$$

From the aluminum test,  $\Delta v/v_0$  may be estimated using the plateau level in the velocity history. An impedance-match calculation, which closely matches a WONDY V modeling using the aluminum EOS from Table 1, gives an expected velocity of 5.035 km/s. The required value of  $\Delta v/v_0$  to match this is  $0.230 \pm 0.047$  (this value was used for the HVL plot in Figure 4). Error estimates here include significant uncertainties (2%) for the LiF and aluminum equations of state, and approximately 1% uncertainty for the projectile velocity. Taking  $n_0 = 1.3939$  and  $\varepsilon_H = 0.4208$ , we conclude that  $n_H = 1.513 \pm 0.034$ . This is plotted together with earlier data and fits [20] in Figure 8.

Hence, the new data are suggestive of a significant change in the optical behavior of LiF in the hypervelocity impact setting. Experiments which include high precision EOS measurements for the target and window material at these stresses will be necessary to determine this optical behavior to better precision.

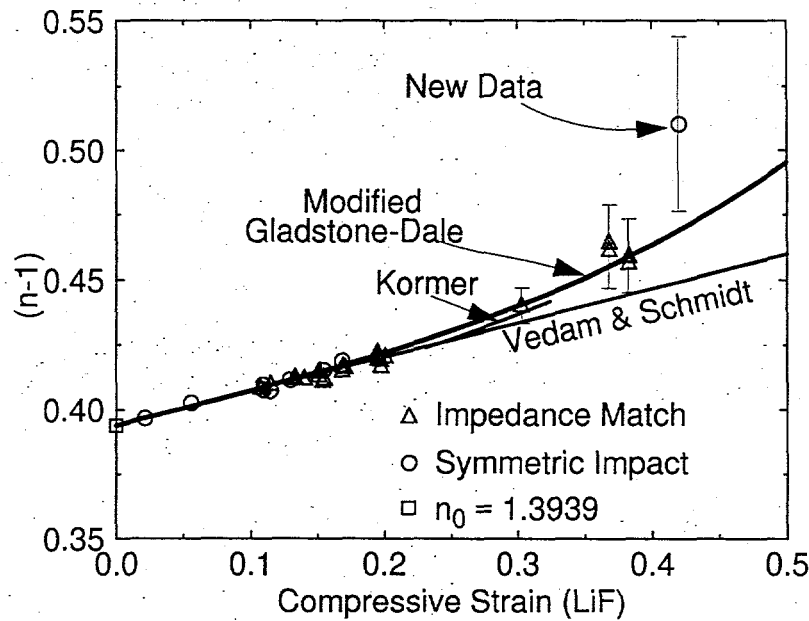


Figure 8. Index of refraction data for LiF. The HVL aluminum-aluminum experiment (L1) lies significantly above the modified Gladstone-Dale curve, with a  $\Delta n/n_0$  value of  $0.23 \pm 0.047$ .

## 5. SUMMARY

The experiments described here demonstrate the use of the hypervelocity launcher to determine material properties in pressure and temperature regimes not previously accessible in the laboratory in the length scales available in plate impact experiments. These are the first time-resolved wave profile measurements on the hypervelocity launcher at impact velocities of 10 km/s. This has allowed the measurements of time-resolved wave profiles for shock loading and release experiments. The experiments presented here illustrate the use of HVL and time-resolved techniques for material properties measurements. These experiments, due to their plate geometry, allow a determination of the EOS of materials, and also serve to validate hydrodynamic codes in the impact regime (where very few experiments are available). Well-controlled EOS studies are necessary for many applications, including ballistic studies [25-26].

Several technical areas must be further developed to allow expanded use of the HVL in planar impact EOS and constitutive property experiments.

Characteristics of the impact process itself (flatness, flyer temperature, and velocity) must be well controlled for increased accuracy, and are amenable to improvement with further HVL development. The experiments discussed here demonstrate the feasibility of such measurements for EOS studies.

Diagnostic issues are also key to experiment usefulness. Window limitations are perhaps the most important barrier for ultra-fast impact experiments if optical probes are to be used. LiF has been seen here to lose transparency at  $\sim 200$  GPa shock pressure, at least for visible (514.5 nm) light. Whether diamond, post-yield sapphire, other salts, or other optical materials with large band gaps could be used at yet higher shock stresses needs to be determined.

It should be emphasized that most of the diagnostic techniques used here are those that were developed earlier for relatively lower impact studies. They need to be refined to give comparable precision with earlier results at more modest regimes. Future studies may benefit from extensions of these techniques (e.g. miniature VISAR probes, improved time resolution in recording, and better) and also from the development of new techniques to better study the physical processes accessible with the hypervelocity launcher.

## REFERENCES

1. L. C. Chhabildas, Int., J. Impact Engng., V5 (1987) 205.
2. L. C. Chhabildas, and R. A. Graham, in AMD Vol. 83, ed., by R. Stout, F. Norwood, and M. Fourney, (1987) 1.
3. See for example LASL Shock Hugoniot Data, ed., by S. P. Marsh, University of California, Press, (1980).
4. J. R. Asay and L. C. Chhabildas, in Shock Waves and High-Strain-Rate Phenomena in Metals, Plenum Publishers, New York (1981).
5. J. R. Asay, L. C. Chhabildas, G. I. Kerley and T. G. Trucano, in *Shock Waves in Condensed Matter-1985*, ed. by Y. M. Gupta, Plenum Publishers, (1986) 145.

6. L. C. Chhabildas, L. M. Barker, J. R. Asay and T. G. Trucano, *Int. J. Impact Engng.*, V10 (1990) 107.
7. L. C. Chhabildas and J. R. Asay in *Shock Waves and High-Strain-Rate Phenomena in Materials*, Marcel Decker, New York (1992) 947.
8. J. R. Asay, T. G. Trucano and L. C. Chhabildas, in *Shock Waves in Condensed Matter-1987*, ed. by S. C. Schmidt, J. W. Forbes and N. C. Holmes, Elsevier Science Publishers, (1988) 159.
9. J. R. Asay, T. G. Trucano and R. S. Hawke, *Int. J. Impact Engng.*, V10, (1990) 51.
10. J. R. Asay and G. I. Kerley, *J. Impact Engng.*, V5, (1987) 69.
11. J. R. Asay, L. C. Chhabildas and L. M. Barker, Sandia National Laboratories Report SAND85-2009, (1985) (unpublished).
12. A. C. Charters, *Int. J. Impact Engng.*, V5 (1987) 181.
13. L. C. Chhabildas, in *Recent Trend in High-Pressure Research*, Proceedings of the XIII AIRAPT Conference on High Pressure Science and Technology, ed. by A. K. Singh, Bangalore, India, (1992) 739.
14. L. M. Barker and R. E. Hollenbach, *J. Appl. Phys.*, 43 (1972) 4669.
15. L. M. Barker, in *Shock Waves in Condensed Matter-1983*, ed. by J. R. Asay, R. A. Graham, and G. K. Straub, Elsevier Science Publishers, (1984) 217.
16. L. C. Chhabildas, L. N. Kmetyk, W. D. Reinhart and C. A. Hall, *Int. J. Impact Engng.*, V17, (1995) 183.
17. L. C. Chhabildas, L. M. Barker, J. R. Asay, T. G. Trucano, G. I. Kerley and J. E. Dunn, in *Shock Waves in Condensed Matter-1991*, ed. by S. C. Schmidt, R. D. Dick, J. W. Forbes and D. G. Tasker, Elsevier Science Publishers, (1992) 1025.
18. L. C. Chhabildas, J. E. Dunn, W. D. Reinhart and J. M. Miller, *Int. J. Impact Engng.*, V14, (1993) 121.
19. J. L. Wise and L. C. Chhabildas, in *Shock Waves in Condensed Matter-1985*, ed. by Y. M. Gupta, Plenum Publishers, (1986) 441.
20. G. I. Kerley, *Int. J. Impact Engng.*, V5, (1987) 441.
21. (e.g.) S. P. Marsh, LASL Shock Hugoniot Data, Univ. of Calif. Press (1980).
22. M. E. Kipp and R. J. Lawrence, WONDY V - A one-dimensional finite-difference wave propagation code, Sandia National Laboratories Report SAND81-0930, 1982.
23. R. G. McQueen, J. N. Fritz, and C. E. Morris, in *Shock Waves in Condensed Matter-1983*, ed. by J. R. Asay, R. A. Graham, and G. K. Straub, Elsevier Science Publishers, (1984) 95.

24. L. C. Chhabildas, W. D. Reinhart and C. A. Hall, Space Programs and Technologies Conference, AIAA Paper 94-4538 (1994).
25. L. C. Chhabildas Hypervelocity Impact Phenomena, *Published in the Metallurgical and Materials Applications of Shock-Wave and High-Strain-Rate Phenomena*, Elsevier Science Publishers, (1995) 245.
26. R. M. Brannon and L. C. Chhabildas, Int., J. Impact Engng., V17, (1995) 109.